Optimization of Spline Slip Surfaces Using Metaheuristic Search in LEM

Terence Ma(✉), Brigid Cami, Sina Javankhoshdel, Brent Corkum, and Thamer Yacoub

Rocscience, 54 St. Patrick St, Toronto, ON M5T 1V1, Canada
terence.ma@rocscience.com

Abstract. The search for the critical slip surface on a slope is an optimization problem whereby the factor of safety is minimized over a set of parameters which define the shape of the slip surface. In limit equilibrium slope stability analysis, traditional methods for searching for the critical slip surface include grid search and auto-refine search. More recently, metaheuristic optimization methods such as Particle Swarm and Cuckoo Search, among other variations, have been used to search for critical slip surfaces. These simulate natural processes that search the solution space for a minimum solution for various optimization problems encountered in a vast range of disciplines. Typically, the parameters of spheres or ellipsoids which cut the ground topography are varied to create different slip surfaces. The parameters of cutting planes and wedges can also be varied to create multi-planar slip surfaces using the same metaheuristic techniques. However, critical slip surfaces are not always spherical, ellipsoidal, or planar in nature. This paper introduces a novel method which employs the use of three-dimensional spline surfaces in a metaheuristic search to find the critical slip surface in a slope. By varying the parameters which define the location, size and curvature of the spline, the critical slip surface can be found. The proposed formulation of parameters is shown to perform better than the parameters which define the preceding shapes due to the superior flexibility of a spline surface in its curvature.

Keywords: Optimization · Slip Surface · Slope Stability · Limit Equilibrium · Critical · Spline · Searching

1 Introduction

Limit equilibrium (LE) is a common method for assessing the overall stability of slopes. For both 2D and 3D slopes, the factor of safety (FS) for a given slip surface below a sliding soil mass can be computed relatively quickly via LE when compared to other common methods such as finite elements (FE). However, a difficulty in LE remains in finding the true FS in a slope, which is governed by the critical slip surface corresponding to the minimum FS. Finding the critical slip surface requires solving an optimization problem wherein the parameters defining the shapes of slip surfaces are varied until the minimum FS is found.

© The Author(s) 2023
S. Javankhoshdel and Y. Abolfazlzadeh (Eds.): TMIC 2022, AHE 13, pp. 130–139, 2023.
https://doi.org/10.2991/978-94-6463-104-3_13

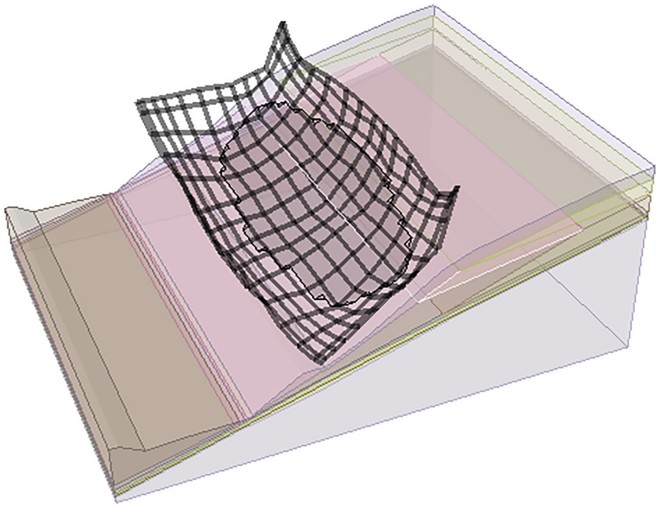

Fig. 1. Example of a spline slip surface defined by a 15x15 grid of points

Particularly in 3D, the FS calculation is relatively expensive compared to 2D so defining an efficient optimization algorithm is required to maintain reasonable computational durations. Traditionally, engineers have relied on simple shapes such as spheres and ellipsoids to define slip surfaces when searching for the minimum FS. Brute search methods such as grid search are still commonly employed, whereby a 3D grid of points is used to spawn the centers of spheres, with varying radii. Smarter methods such as auto-refining algorithms have intensified the searching in regions with lower FS. Still further, metaheuristic optimization algorithms such as Particle Swarm Optimization (PSO) and Cuckoo Search have been used to determine the minimum FS of slip surfaces in slopes. These have received widespread acceptance in slope stability research [1–10] due to their ability to simulate natural processes to converge to a minimum FS slip surface relatively quickly.

Many commercial slope stability programs offer the option to search for simple types of surfaces, such as spheres, ellipsoids, and planar surfaces. These shapes are easy to define as inputs into the above methods but suffer from lack of accuracy and ability to represent the true critical slip surface in a slope because they are inflexible. Recently, a Surface Altering (SA) optimization has been proposed for 3D slopes [5], which can approximate the minimum FS result from the metaheuristic search of these primitive surfaces (e.g. the minimum FS ellipsoid) into a plan-rectangular array of spline points. The spline points form a net in 3D over which a Non-Uniform Rational Basis Spline (NURBS) surface is contained, and its points can be manipulated to alter the slip surface locally to find the minimum FS. In Fig. 1, a 15 by 15 grid of points is shown, and the actual slip surface marked as the intersection of the spline surface with the slope geometry is shaded.

The SA approach can technically approximate any slip surface obtained from the metaheuristic search, and locally minimizes the FS. However, the approximation suggested by [5] can cause undesirable changes to the geometry of the slip surface and can

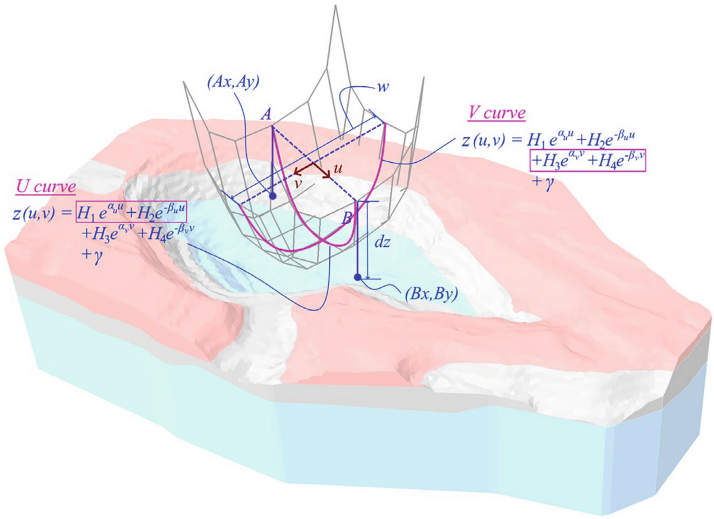

Fig. 2. Parameters defining the proposed spline surface

increase the FS obtained from the approximated surface before the local optimization is performed. Furthermore, the minimum FS ellipsoid or sphere in a slope may not be in the correct location, due to the inflexibility of the shape used during the metaheuristic search. This paper proposes a method whereby the metaheuristic search can be conducted using spline surfaces directly, which increases the flexibility of the shapes being searched and does not require approximation when inputting the minimum surface into SA.

2 Methodology

Ellipsoids, spheres, and other shapes used in the metaheuristic search can all be defined using a list of parameters which can be varied. For example, a sphere can be defined using four parameters, consisting of a center point (3 parameters – *x, y* and *z* in 3D space) and radius. An ellipsoid can be defined using some additional parameters corresponding to the principal radii and rotations. These parameters are varied using a metaheuristic algorithm such as PSO to minimize the FS. Other metaheuristic algorithms can be used, but PSO will be used to produce the results in this paper since it is among the most popular. Details of the original PSO algorithm can be found in [11].

The proposed parameters defining the spline slip surface form are shown in Fig. 2. There are eleven parameters in total, which define the general size and location of the surface, and the curvature in the two orthogonal plan directions. Table 1 provides a list of the parameters and their descriptions.

The creation of a spline surface using values of these eleven parameters is described as follows. First, points *A* and *B* are spawned at random locations within the plan extents of the model. A local coordinate system (LCS) is defined whereby *u* is a vector originating from the midpoint of *AB* and pointing in the direction of *B*. The other local coordinate

Table 1. List of parameters in the proposed spline metaheuristic search.

A_x	X coordinate of Point A
A_y	Y coordinate of Point A
B_x	X coordinate of Point B
B_y	Y coordinate of Point B
w	Width of the control net in the v direction
dz	Elevation offset of Point A above the ground elevation at (A_x, A_y)
γ	Reference floor elevation of the spline surface
α_u	Positive skew in the u direction
β_u	Negative skew in the u direction
α_v	Positive skew in the v direction
β_v	Negative skew in the v direction

axis, the v direction, is the cross product of u and the z axis. Then an exponentially curved surface in these two directions is defined via Eq. 1.

$$z(u, v) = H_1 e^{\alpha_u u} + H_2 e^{-\beta_u u} + H_3 e^{\alpha_v v} + H_4 e^{-\beta_v v} + \gamma \tag{1}$$

The coefficients H_1 through H_4 are given in Eq. 2

$$H_1 = \frac{-e^{\alpha_u}\left(C_1 + \gamma\left(e^{2\beta_u} - 1\right)(e^{\alpha_v} - 1)\left(e^{\beta_v} - 1\right)\right)}{D\left(e^{\alpha_u + \beta_u} - 1\right)} \tag{2a}$$

$$H_2 = \frac{-e^{\beta_u}\left(C_2 + \gamma\left(e^{2\alpha_u} - 1\right)(e^{\alpha_v} - 1)\left(e^{\beta_v} - 1\right)\right)}{D\left(e^{\alpha_u + \beta_u} - 1\right)} \tag{2b}$$

$$H_3 = \frac{-e^{\alpha_v}\left(C_3 + \gamma\left(e^{2\beta_v} - 1\right)(e^{\alpha_u} - 1)\left(e^{\beta_u} - 1\right)\right)}{D\left(e^{\alpha_v + \beta_v} - 1\right)} \tag{2c}$$

$$H_4 = \frac{-e^{\beta_v}\left(C_4 + \gamma\left(e^{2\alpha_v} - 1\right)(e^{\alpha_u} - 1)\left(e^{\beta_u} - 1\right)\right)}{D\left(e^{\alpha_v + \beta_v} - 1\right)} \tag{2d}$$

$$C_1 = \left(A_z - B_z e^{2\beta_u}\right)\left(1 + e^{\alpha_v + \beta_v}\right) + \frac{A_z + B_z}{2}\left(e^{\alpha_v} + e^{\beta_v}\right)\left(e^{2\beta_u} - 1\right) - (A_z - B_z)e^{\beta_u}\left(e^{\alpha_v} + e^{\beta_v}\right) \tag{2e}$$

$$C_2 = \left(B_z - A_z e^{2\alpha_u}\right)\left(1 + e^{\beta_v + \alpha_v}\right) + \frac{B_z + A_z}{2}\left(e^{\beta_v} + e^{\alpha_v}\right)\left(e^{2\alpha_u} - 1\right) - (B_z - A_z)e^{\alpha_u}\left(e^{\beta_v} + e^{\alpha_v}\right) \tag{2f}$$

$$C_3 = \left(e^{2\beta_v} - 1\right)\left(A_z e^{\alpha_u} + B_z e^{\beta_u} - \frac{A_z + B_z}{2}\left(e^{\alpha_u + \beta_u} + 1\right)\right) \tag{2g}$$

$$C_4 = \left(e^{2\alpha_v} - 1\right)\left(A_z e^{\alpha_u} + B_z e^{\beta_u} - \frac{A_z + B_z}{2}\left(e^{\alpha_u + \beta_u} + 1\right)\right) \tag{2h}$$

$$D = 1 + e^{\alpha_u + \alpha_v + \beta_u + \beta_v} + e^{\alpha_u + \beta_u} + e^{\alpha_v + \beta_v} - e^{\alpha_u + \alpha_v} - e^{\beta_u + \beta_v} - e^{\alpha_u + \beta_v} - e^{\alpha_v + \beta_u} \tag{2i}$$

The H coefficients are defined such that they map the LCS points into global space via Eq. 3

$$A_Z = Z(-1, 0) \tag{3a}$$

$$B_Z = Z = (+1, 0) \tag{3b}$$

$$0.5(A_z + B_z) = z(0, -1) \tag{3c}$$

$$0.5(A_z + B_z) = z(0, +1) \tag{3d}$$

The function in Eq. 1 is also scaled in global space such that the plan width w exists between any two points in the v direction, (u, 1) and (u, −1). After the exponential surface is defined, spline points are spawned on the exponential surface at locations of u and v equal to {−1.1, −1.0, −0.9, −0.8, −0.5, 0, 0.5, 0.8, 0.9, 1.0, 1.1}. This configuration results in an 11 by 11 grid of control points forming a NURBS surface. The locations and number of these points in each direction can be changed. For this paper, the NURBS surfaces have a degree of 2, and the knot vectors are uniform and clamped. The end points have weights 0.1, while inner points have weights 1.0. A full description of NURBS surfaces can be found in [12]. The resulting NURBS will have a slightly different geometry from the exponential surface.

The PSO search is accomplished by varying these eleven parameters to find the minimum slip surface. After the global minimum is found, the NURBS surface can be directly inputted into the SA algorithm without requiring approximation. However, the NURBS surface can be refined to have more control points without altering the resulting geometry of the NURBS surface via the curve refinement procedures described in [12]. It can also be trimmed via curve splitting [12] such that only the portion of the NURBS surface intersecting the ground topography is considered. This way, large parts of the NURBS surface above the ground topography can be discarded before SA occurs to ensure greater efficiency during the local optimization.

3 Numerical Example

In the following example, the results of an ellipsoidal PSO search with and without SA are compared with the results of the proposed spline PSO search with and without SA. The example, illustrated in Fig. 3, is of a slope in a coal mine adopted from a verification manual [13] for 3D slopes. It contains anisotropic material properties, defined in the original source, and listed in Tables 2 and 3.

In Tables 2 and 3, the Mohr-Coulomb parameters c' and ϕ correspond to the cohesion and friction angle, respectively. γ_d is the unit weight, and A and B are the angle ranges of the joints in the respective dip and dip directions. For the Jointed CMR rock mass, if the slipping vector at the base of a column in the slip surface is within A degrees of the closest joint, then the joint material is applied to the base of the column. If it is between A and B then a linear interpolation is applied to the shear strength between the joint and base materials. If it is beyond B then the base material (Fresh CMR) applies.

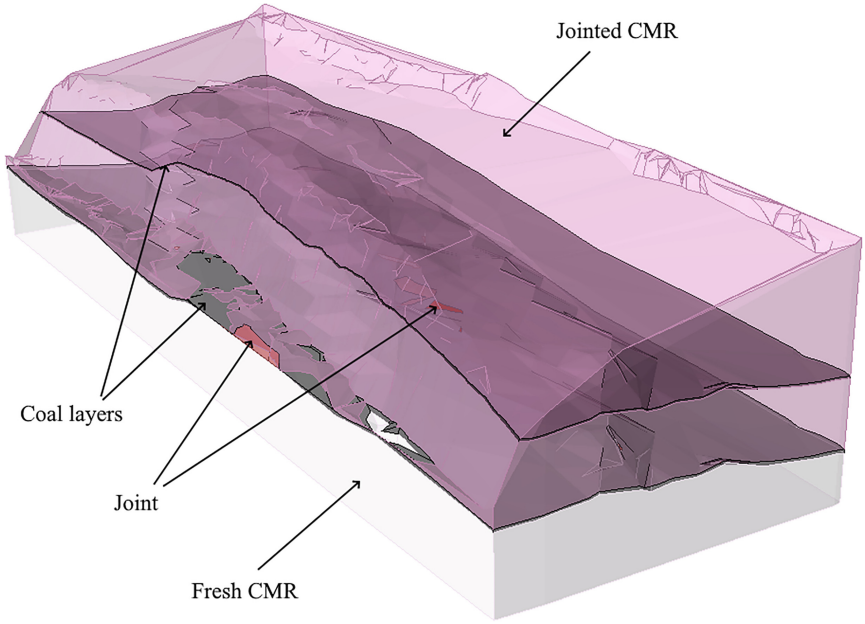

Fig. 3. Example of a coal mine with anisotropic materials

Table 2. Material properties for Mohr-Coulomb properties in coal mine example

Layer	c' (kPa)	ϕ (°)	γ_d [kN/m^3]
Joint	2	12	15
Coal layers	35	30	15
Fresh CMR	120	30	24

Table 3. Material properties for the anisotropic material layer in coal mine example.

Layer	γ_d [kN/m^3]	Base Material	Joint Material	Dip	Dip Direction	A	B
Jointed CMR	20	Fresh CMR	Joint	81°	132°	5°	10°
				74°	49°	5°	10°

In Table 4, the results of the proposed method with PSO search are compared with the results of the ellipsoid search with PSO obtained from Slide3 (version 3.018). The Spencer FS reported in each cell is the result obtained from starting the metaheuristic algorithm with a different random seed. In the end, the results from five seeds are averaged to give the value F^* corresponding to the method used. Taking the average provides a

Table 4. Comparison between ellipsoid and spline search results (Spencer FS) for coal mine example.

	Ellipsoid Search	Spline Search	Ellipsoid Search + 3D SA	Spline Search + 3D SA
FS (Seed 1)	1.219	1.172	1.177	1.140
FS (Seed 2)	1.230	1.154	1.179	1.133
FS (Seed 3)	1.228	1.195	1.178	1.149
FS (Seed 4)	1.208	1.133	1.165	1.115
FS (Seed 5)	1.219	1.166	1.187	1.110
Average (F^*)	**1.221**	**1.164**	**1.177**	**1.129**

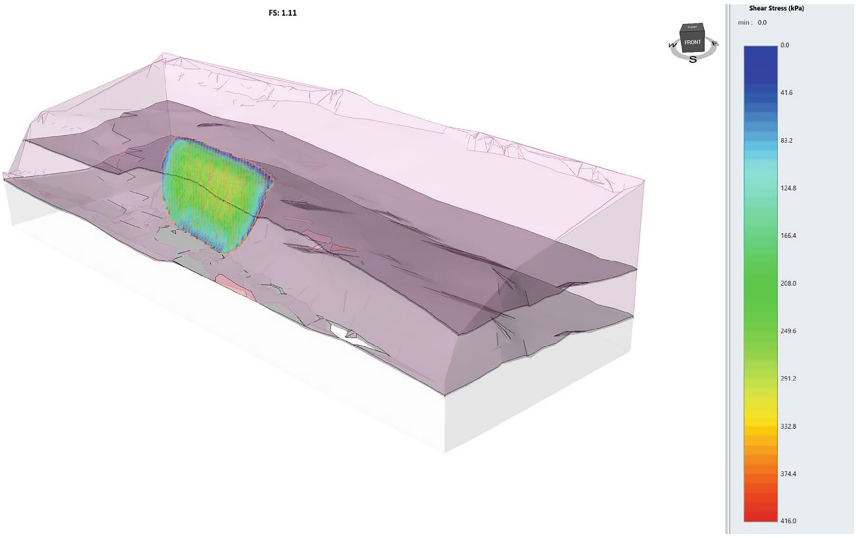

Fig. 4. Global minimum Spencer FS = 1.11 result obtained from all the searches and seeds

more reliable assessment of whether either of the methods is truly and consistently better than the other.

Figure 4 shows the global minimum result (FS = 1.11) obtained from all the searches, found during the SA after the spline search on Seed 5. Figure 5 shows the corresponding grid of control points which were used to generate the surface.

From the results of Table 4, the spline search alone ($F^* = 1.164$) was superior to the ellipsoid search ($F^* = 1.221$), and even outperformed the post-SA results of the

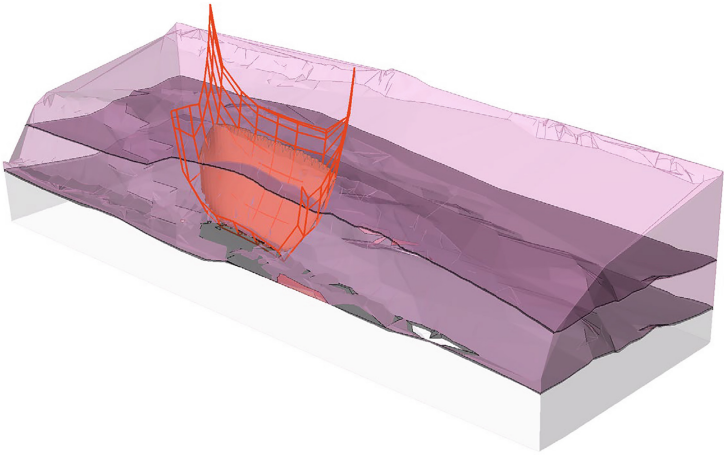

Fig. 5. Grid of spline points used to generate the global minimum surface

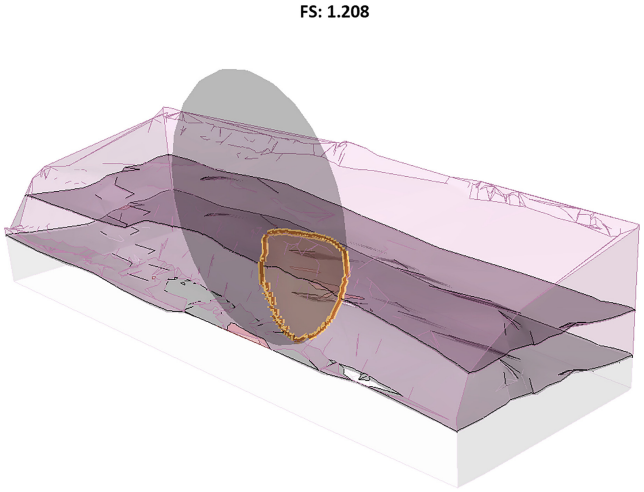

Fig. 6. Global minimum ellipsoid Spencer FS = 1.208

ellipsoid search ($F^* = 1.177$). For comparison, the minimum ellipsoid was found in Seed 4 and as shown in Fig. 6, is not in the same location as the true global minimum slip surface. When SA was performed on this ellipsoidal surface, a minimum FS of 1.165 was obtained after the local optimization, shown in Fig. 7 with the corresponding grid of spline points. Clearly, it is in a different location from the true global minimum found by the spline search result with surface altering.

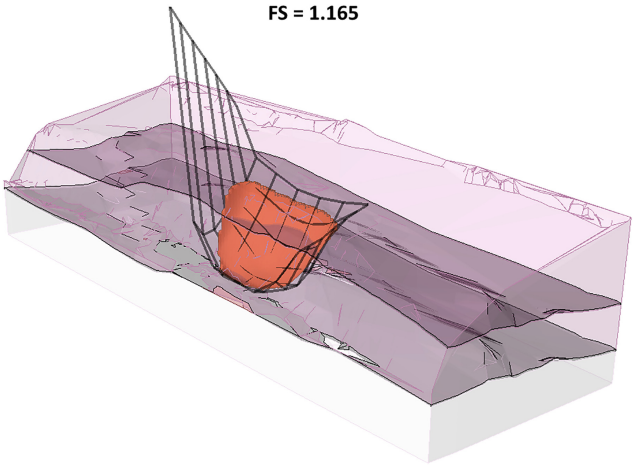

Fig. 7. After altering the 1.208 ellipsoid surface, a local minimum FS of 1.165 was obtained

4 Conclusions

A new method for metaheuristic searching of slip surfaces is introduced, which involves using spline surfaces instead of the conventional ellipsoidal and spherical slip surfaces. The method allows for much more flexibility in the shapes of the slip surfaces that are produced during the search and can be readily used as an input to the surface altering algorithm, rather than requiring an approximation. As such, the proposed method is more reliable at searching for the true critical slip surface in a slope than its predecessors. As demonstrated in the example, due to the relative inflexibility of ellipsoid and spherical slip surfaces, it is possible for ellipsoidal and spherical searching to converge to a region containing a local minimum FS which is different from the true global minimum.

References

1. Cheng, Y.M., Liu, H.T., Wei W.B., and Au, S.K. 2005. Location of critical three-dimensional non-spherical failure surface by NURBS functions and ellipsoid with applications to highway slopes. Comput Geotech. 32(6): 387–399.
2. Jiang, J.C., Yamagami, T., and Baker, R. 2003. Three-dimensional slope stability analysis based on nonlinear failure envelope. Chinese J Rock Mech and Eng, 22(6): 1017–1023.
3. Kalatehjari, R., A Rashid, A. S., Ali, N., and Hajihassani, M. 2014. The contribution of particle swarm optimization to three-dimensional slope stability analysis. The Scientific World Journal.
4. Kalatehjari, R., Ali, N., Hajihassani, M., and Fard M.K., 2012. The application of particle swarm optimization in slope stability analysis of homogeneous soil slopes. International Review on Modelling and Simulations, 5(1): 458–65.
5. Ma, T., Mafi, R., Cami, B., Javankhoshdel, S., Gandomi, A.H. (2022). NURBS surface-altering optimization for identifying critical slip surfaces in 3D slopes. Int. J. Geomech.
6. Mowen, X.J.E. 2004. A simple Monte Carlo method for locating the three-dimensional critical slip surface of a slope. ActaGeologica Sinica. 78(6): 1258–66.

7. Mowen, X.J.E., Zengfu, W., Xiangyu, L., and Bo, X. 2011. Three-dimensional critical slip surface locating and slope stability assessment for lava lobe of Unzen Volcano. J Rock Mech and Geotech Eng, 3(1): 82–89.
8. Su, Z., & Shao, L. 2021. A three-dimensional slope stability analysis method based on finite element method stress analysis. Engineering Geology, 280, 105910.
9. Toufigh, M., Ahangarasr, A., and Ouria, A. 1995. "Using non-linear programming techniques in determination of the most probable slip surface in 3D slopes," World Academy of Science, Engineering and Technology, vol. 17, pp. 30–35, 2006. on Micro Machine and Human Science, pp. 39–43, IEEE, Nagoya, Japan, October 1995.
10. Yamagami, T., and Jiang, J.C. 1997. A search for the critical slip surface in three-dimensional slope stability analysis. Soils and Foundations, 37(3): 1–16.
11. Kennedy, J. 2007. Some issues and practices for particle swarms. In Proceedings of the 2007 IEEE Swarm Intelligence Symposium (SIS 2007).
12. Piegl, L., and Tiller, W. 1997. The NURBS Book (2nd ed.). Springer-Verlag, Berlin, Heidelberg.
13. Rocscience. 2022. 3D Verification. https://static.rocscience.cloud/assets/verification-and-theory/Slide3/Slope-Stability-Verification-3D.pdf, last accessed August 1, 2022.

Open Access This chapter is licensed under the terms of the Creative Commons Attribution-NonCommercial 4.0 International License (http://creativecommons.org/licenses/by-nc/4.0/), which permits any noncommercial use, sharing, adaptation, distribution and reproduction in any medium or format, as long as you give appropriate credit to the original author(s) and the source, provide a link to the Creative Commons license and indicate if changes were made.

The images or other third party material in this chapter are included in the chapter's Creative Commons license, unless indicated otherwise in a credit line to the material. If material is not included in the chapter's Creative Commons license and your intended use is not permitted by statutory regulation or exceeds the permitted use, you will need to obtain permission directly from the copyright holder.